Investigations of Rydberg-Atom Based THz-Wave Electric Field Sensor

Motohiro Kumagai, Shigeo Nagano
Space-Time Standards Group
National Institute of Information and Communications Technology (NICT)
Tokyo, JAPAN
mkumagai@nict.go.jp

Shin'ichiro Hayashi, Norihiko Sekine
Terahertz Technology Research Center
National Institute of Information and Communications Technology (NICT)
Tokyo, JAPAN

We have started research on Rydberg-atom based sensor, which is capable of SI-traceable electric field measurements of Terahertz waves. The ladder-type EIT (Electromagnetically Induced Transparency) signals were prepared by counterpropagating lasers of two distinct wavelength lasers corresponding to the S-P-D transitions of Cesium (Cs) atoms enclosed in a cylindrical glass cell. Irradiation of a THz-wave whose frequency matched the D-F transition then results in an observed Autler-Townes (AT) splitting of the EIT signal. We confirmed that the frequency separation of the splitting changes with the irradiated power of the 100GHz and 300 waves.

Keywords—SI-traceable, electrometry, Terahertz wave, Autler-Townes splitting

I. INTRODUCTION

With the technological growth in various scientific and industrial field an application using a higher frequency electromagnetic wave is increasing. Especially Terahertz waves have been recently used for several applications in high-speed wireless communication, nondestructive sensing and imaging or astrophysics. To take full advantage of high frequency sources NICT has been conducting research of frequency metrology in the THz band [1,2]. In addition to accurate frequency allocations highly sensitive and robust measurements for electromagnetic field strength of the waves are also in demand. Rydberg-atom based electric field sensors are expected to act as an SI-traceable electrometer surpassing calorimeters or antennas in providing simple and accurate measurements. Various results and applications have already been reported [3-9]. NICT has started research of Rydberg-atom sensors for the THz band to leverage the synergies of frequency metrology and electrometry.

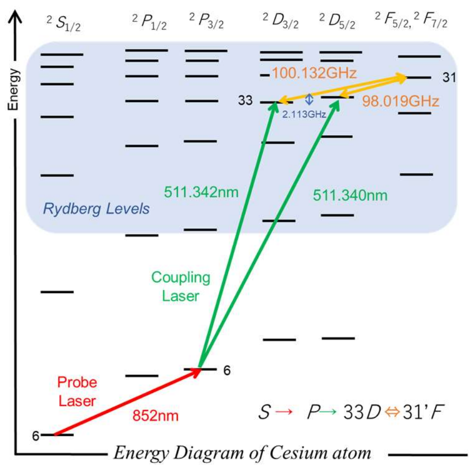

Figure 1. Energy levels of Cs atom and target transitions for the 100GHz wave measurement

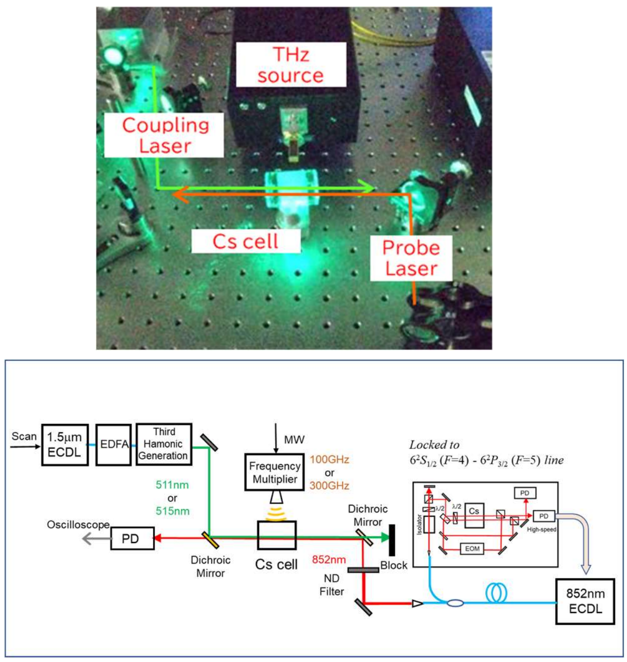

Figure 2. Photo and simplified experimental setup for Rydberg-atom based THz-wave electric field sensor

II. EXPERIMENTAL SETUP

Figure 1 shows the energy levels of the Cs atom used for the 100GHz wave measurement, where a 852nm probe laser excites the atom from the 6*S* ground state to the 6*P* state and a 511nm coupling laser is used to transfer the excited atom from the 6*P* state to a specific Rydberg 33*D* state. The 852nm laser light is emitted by a conventional external-cavity diode laser (ECDL), whereas the 511nm laser light is supplied from 1.5μm ECDL by the third harmonics generation using one module including two periodically-poled lithium niobate (PPLN) waveguides for second harmonic generation and sum frequency generation [10]. The conversion efficiency of the PPLN module is about 100%/W^2. The 852nm and the 511nm lasers counter-propagate through a glass cell filled with Cs vapor, with an optical power of about 100μW and 20mW, respectively. The laser beam diameter is about 2mm. In this experiment, the laser frequency of the 852nm external-cavity diode laser (ECDL) is locked to the $6^2S_{1/2}$ (F=4) - $6^2P_{3/2}$ (F=5) transition of the D_2 line. The 511nm laser frequency is scanned for measurement of the ladder-type EIT signal of the 6S-6P-33D transition. The presence of THz-wave resonant with the energy difference between the D state and a neighboring Rydberg F state can then induce the AT splitting [11] of the EIT signal. The frequency separation corresponds to the Rabi frequency, which is determined by the dipole moments of the transition and the electric field of the irradiated THz-wave. This electric field can thus be obtained by careful measurements of the frequency splitting.

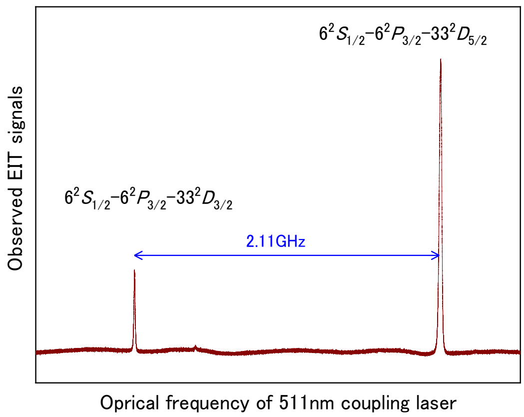

Figure 3. Observed EIT signals when the 852nm probe laser is locked to the D_2 line and the 511nm coupling lased is scanned over 3GHz

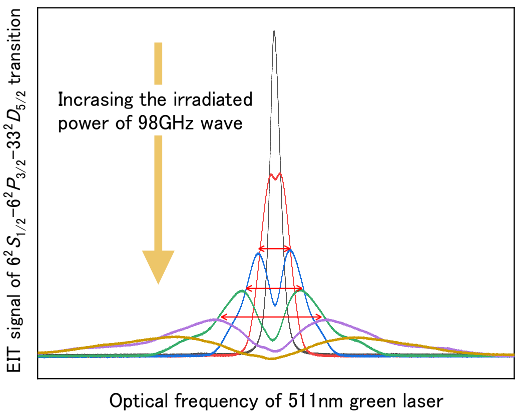

Figure 4. AT splitting of EIT signal with increasing the power of the 98GHz

III. Measurement of AT-Splitting by a 100GHz wave

Figure 3 shows the observed EIT signals for a wide scan of the coupling laser. The two peaks correspond to the $6^2S_{1/2}$ - $6^2P_{3/2}$ - $33^2D_{3/2}$ and $6^2S_{1/2}$ - $6^2P_{3/2}$ - $33^2D_{5/2}$ transitions. According to numerical calculations [12], the fine structure energy difference of 33D is about 2.11GHz. No information is available about the hyperfine structures. The hyperfine states can likely be considered to be degenerate.

We then irradiate the 100GHz wave corresponding to the energy difference between 33D and 31F states. This is generated as the 6th harmonic of a microwave source and the maximum irradiated power is about 20mW. Figure 4 shows the behavior of the EIT signal of the $6^2S_{1/2}$ - $6^2P_{3/2}$ - $33^2D_{5/2}$ transition for increasing THz-wave power irradiated on the intersection of the laser beams. We can see that the splitting widens with increasing irradiated power. The frequency of the irradiated THz-wave is 98GHz, corresponding to the $33^2D_{5/2}$-$31^2F_{7/2,\,5/2}$ transition.

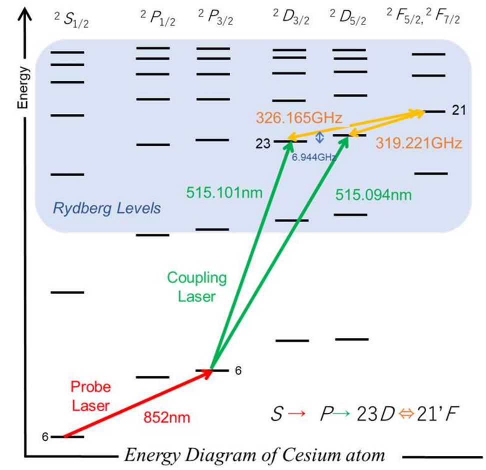

Figure 5. Energy levels of Cs atom and target transitions for the 300GHz wave measurement

IV. Measurement of AT-Splitting by a 300GHz wave

The energy levels of the Cs atom for the 300GHz wave measurements are shown in Fig. 5. To transfer the excited atom in the 6P state to a Rydberg 23D state, another PPLN module for the third harmonic generation was replaced and the 1.5 mm ECDL was frequency-tuned for the 515 nm green light generation. The 300 GHz wave source was prepared by attaching a tripler onto the 100GHz source, The output power was about 1mW at maximum. Similar to the 100GHz wave measurements, two EIT signals of the S-P-$D_{3/2}$ and the S-P-$D_{5/2}$ transitions were observed in Figure 6. The frequency difference of two signal is 6.944 GHz. When we irradiate the 320GHz waves corresponding to the energy difference between 23D and 21F states, the AT-splitting was observed on each EIT signal, and it widens with increasing the irradiated THz-wave power.

The dipole moment of the 23D-21F transition for the 300GHz wave measurement is smaller than that of the 33D-31F transition for the 100GHz wave. Furthermore, the output power of the 300GHz wave source is lower than that of the 100GHz wave source. These limit the splitting broadening of the EIT signals. Optimizing the THz wave coupling to the intersection of the laser beams would increase the widening of the AT-splitting.

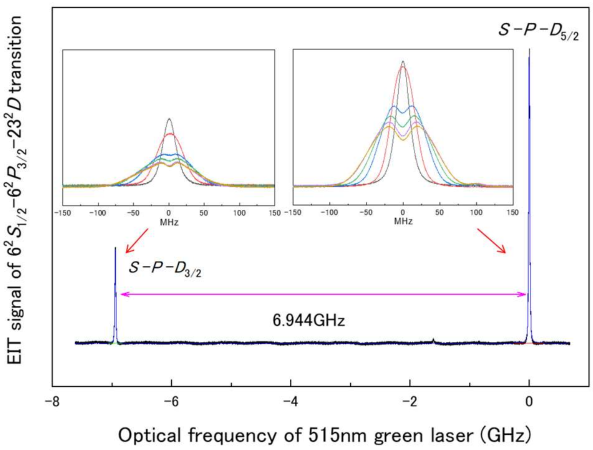

Fig.6. Observed EIT signals when the 852nm probe laser is locked to the D_2 line and the 515nm coupling lased is scanned over 8GHz. (Inset) AT-splitting of the EIT signals when the 320GHz wave resonant to each *D-F* transition is irradiated onto the Cs cell.

V. Summary and Future Plan

In our preliminary experiments, very simple measurement setup using one Cs gas cell and two lasers was prepared and we have succeeded in observing the AT splitting of the EIT signal caused by a 100GHz wave and a 300GHz wave. We also confirmed that the splitting widens with increasing irradiated THz-wave power. This becomes the first step toward the accurate electrometer for the THz-wave. As the next step, the actual measurements of the electric field strength of the irradiated THz-wave and their accuracy evaluation are planned.

References

[1] H. Ito, S. Nagano. M.Kumagai. M. Kajita and Y. Hanado, “Terahertz Frequency Counter with a Fractional Frequency Uncertainty at the 10^{-17} Level,” Appl. Phys. Express 6, 1022021, 2013.

[2] S. Nagano. M.Kumagai. H. Ito, Y. Hanado and T. Ido, “Terahertz frequency counter based on a semiconductor-superlattice harmonic mixer with four-octave measurable bandwidth and 16-digit precision,” Metrologia 58, 055001, 2021.

[3] S. Kumar, H. Fan, H. Kübler, A. J. Jahangiri, and J. P. Shaffer, "Rydberg-atom based radio-frequency electrometry using frequency modulation spectroscopy in room temperature vapor cells," Opt. Express 25, 8625-8637, 2017

[4] J. A. Gordon, M. T. Simons, A. H. Haddab, and C. L. Holloway, “Weak electric field detection with sub-1 Hz resolution at radio frequencies using a Rydberg atom-based mixer,” AIP Adv., vol. 9, no. 4, 2019.

[5] C. T. Fancher, D. R. Scherer, M. C. S. John and B. L. S. Marlow, "Rydberg Atom Electric Field Sensors for Communications and Sensing," in IEEE Transactions on Quantum Engineering, vol. 2, pp. 1-13, 2021.

[6] C. L. Holloway et al, “A quantum-based power standard: Using Rydberg atoms for a SI-traceable radio-frequency power measurement technique in rectangular waveguides” *Appl. Phys. Lett.* 113, 09410, 2018

[7] C. Holloway et al., “A multiple-band Rydberg atom-based receiver: AM/FM stereo reception,” IEEE Antennas Propag. Mag., 63(3), 63-76, 2020

[8] Nikunjkumar Prajapati, et al, “Enhancement of electromagnetically induced transparency based Rydberg-atom electrometry through population repumping”. *Appl. Phys. Lett.* 119, 214001, 2021

[9] S. Chen et al, "Terahertz electrometry via infrared spectroscopy of atomic vapor," Optica 9, 485-491, 2022)

[10] Philippe, C., Chea, E., Nishida, Y. et al. “Efficient third harmonic generation of a CW-fibered 1.5 µm laser diode”. Appl. Phys. B 122, 265 2016

[11] S. H. Autler and C. H. Townes, “Stark Effect in Rapidly Varying Fields,” Phys. Rev. 100, 703, 1955.

[12] N. Šibalić, J.D. Pritchard, C.S. Adams and K.J. Weatherill, “ARC: An open-source library for calculating properties of alkali Rydberg atoms,” Computer Physics Communications, 220, 319, 2017.